



Barium and strontium doped La-based perovskite synthesis via sol-gel route and photocatalytic activity evaluation for methylene blue

Sadia Ata^a, Ifra Shaheen^a, Hira Aslam^a, Ijaz Ul Mohsin^b, Norah Alwadai^c, Maryam Al Huwayz^c, Munawar Iqbal^{d,*}, Umer Younas^{e,*}

^a School of Chemistry, University of the Punjab, Lahore, Pakistan

^b Institute of Applied Materials-Applied Materials Physics (IAM-AWP), Karlsruhe Institute of Technology, Karlsruhe, Germany

^c Department of Physics, College of Sciences, Princess Nourah bint Abdulrahman University, P.O. Box 84428, Riyadh 11671, Saudi Arabia

^d Department of Chemistry, Division of Science and Technology, University of Education, Lahore, Pakistan

^e Department of Chemistry, The University of Lahore, Lahore, Pakistan

ARTICLE INFO

Keywords:

Perovskite
Ba and Sr doping
Sol-gel synthesis
Photocatalytic activity
Dielectric properties
AC conductivity

ABSTRACT

In the current work, a La-based nanocomposite ($\text{La}_x\text{Ba}_{1-x}\text{Sr}_y\text{Cd}_{1-y}\text{O}_{3\pm\delta}$) has been synthesized via sol-gel method. The influence of Ba and Sr doping on the structural, dielectric and photocatalytic characteristics of La-based perovskite nanocomposite has been investigated. The synthesized material was characterized employing different techniques such as FTIR, XRD, which confirmed the formation of nanocomposite. Representative peaks of metal oxygen bonds (M–O), in FTIR spectra confirmed the formation of the product. Orthorhombic crystalline structures having particle size 89.92 nm was confirmed by XRD analysis. Dielectric studies were conducted for the synthesized nanocomposite. The real and imaginary dielectric constant exhibited conservation and consumption of energy and AC conductivity analysis elaborated the effect of frequency on conductivity of the synthesized sample. Doping of nanomaterial with Ba and Sr caused inhomogeneity in the structure that caused reduction in number of moving charges due to which dielectric constant was found maximum at lower frequency. Enhanced dielectric properties caused a decrement in energy losses with increasing frequency. The results of AC conductivity were found directly related to frequency that may be due to enhanced charge storage capacity of perovskite after doping. In addition, synthesized nanoparticles exhibited excellent photocatalytic activity for the degradation of methylene blue (5 ppm). Under optimized conditions of pH, catalyst dose and UV light, 89.92% degradation of dye was achieved in 65 min. It is concluded that the synthesized nanomaterial i.e. Ba and Sr doped Lanthanum Perovskites can be a potent candidate for photocatalytic applications.

Introduction

Increase of environmental pollution at massive level due to effluents containing toxic pollutants, discharged by different industries, may pose multiple hazardous health effects [1,2]. Among these pollutants, organic compounds such as azo dyes (methylene blue and methylene orange) have now become very crucial due to their deleterious effects on environment and human health [3]. Aromatic azo dyes constitute half of total amount of the dyes produced and used in world. These dyes are being used in different industries and 15% of the used dyes are being discharged in waterbodies [4]. Azo dyes are potential carcinogenic [5], allergic to eyes and skin and may also cause respiratory problems [6]. These contaminants are being generally removed employing different

methods such as biodegradation, chlorination, flocculation, ozonation, photochemical oxidation and researchers are still focusing in developing environment friendly and economical methods for the removal of dyes [7]. Photocatalytic degradation methodology is an environment friendly method that produces less harmful products. This technique relies on the interaction of radiation with a surface of nanocatalyst and oxidative reagents are formed as a result degradation of many contaminants take place [8,9]. Recently, photocatalytic activity of perovskite-type oxides has gotten appreciable attention due to their economical, have high catalytic ability, and environmental adaptability [10].

Huge consumption of non-renewable energy resources has become a serious threat for the environment, being against the sustainable development goals set by united nation. There is a dire need to develop

* Corresponding authors.

E-mail addresses: bosalvee@yahoo.com (M. Iqbal), umer0608analyst@gmail.com (U. Younas).

<https://doi.org/10.1016/j.rinp.2023.106235>

Received 19 November 2022; Received in revised form 16 January 2023; Accepted 18 January 2023

Available online 21 January 2023

2211-3797/© 2023 The Authors. Published by Elsevier B.V. This is an open access article under the CC BY license (<http://creativecommons.org/licenses/by/4.0/>).

low cost, efficient, less hazardous materials for energy storage devices [11]. Supercapacitors have received much attention of researchers due to the advantages including long life-cycle, high power density, fast charge and discharge speed. Low energy density is a problem that has restricted their commercial application. Thus, development of materials with improved energy density of supercapacitor has become an important issue [12]. Electrode material is the basic component that responsible for electrochemical performance of a supercapacitor. Researchers are now focusing on the development of high performance electrode materials and perovskites found to be a promising candidate [13].

General formula of perovskites is ABX_3 , where A or B site carry metal ions. Substitution of selected metal at position A or B has been reported and such substitutions can strongly influence the properties of perovskites [14]. Modifications in structural, catalytic, electrochemical activities of perovskite materials have been achieved by introducing different metals at position A and B [15,16]. In the light of previous reports, it is observed that the doping is a useful tool to enhanced the activity of the doped material, which is because of reduction in the bandgap as well as the optical and physicochemical properties of the doped materials [17]. The Mn and Co-based perovskites showed promising photocatalytic activity for oxidation reaction [18–20]. Mostly Lanthanum based perovskites such as LaMnO_3 have been reported for their promising photocatalytic applications. Ghiasi, M. et al. (2014) reported synthesis of LaSrMnO_3 [21] and Esmaeili et al. (2020) reported the formation of LaBaMnO_3 for the degradation of methyl orange in UV and sunlight [22]. Advancements in designing and synthesis of novel nanocomposites especially perovskite are being reported. Scientists are making efforts to synthesize nanocomposite with appropriate composition with maximum photocatalytic and charge storage potential. Still, there is need to synthesize perovskite based nanomaterials with novel composition.

The La-based perovskites nanomaterials can be synthesized by different methods such as hydrothermal [23], reverse-phase hydrolysis [24], co-precipitation [25], microwave assisted methods [26] and solid-state reaction [27]. Sol-gel is one of the easiest methods that can be used for the manufacturing of high quality nanoparticles [28]. This method is easy, cost effective and helpful in inducing certain properties such as control over size, morphology and many electrochemical properties [29]. In this paper, we have reported the synthesis of Ba and Sr doped La-based perovskite nanocomposite LaBaSrCdO_3 ($\text{La}_x\text{Ba}_{1-x}\text{Sr}_y\text{Cd}_{1-y}\text{O}_3 \pm \delta$) by sol-gel method. Photocatalytic degradation of methylene blue using synthesized nanocatalyst has also been achieved under UV light employing different conditions of pH and catalyst dose. In addition,

dielectric studies have been carried out to determine its potential for supercapacitor applications. Current study will be helpful in designing and synthesis of perovskite type nanomaterials with enhanced properties.

Experimental

Material

Lanthanum nitrate ($\text{La}(\text{NO}_3)_3 \cdot 6\text{H}_2\text{O}$), strontium chloride ($\text{SrCl}_2 \cdot 6\text{H}_2\text{O}$), cadmium nitrate ($\text{Cd}(\text{NO}_3)_2 \cdot 4\text{H}_2\text{O}$), barium chloride ($\text{BaCl}_2 \cdot 2\text{H}_2\text{O}$), citric acid ($\text{C}_6\text{H}_8\text{O}_6$), ammonium hydroxide (NH_4OH) 10 % w/w sodium hydroxide (NaOH), hydrochloric acid (HCl), ethanol, Methylene blue and distilled water were used and all the chemical reagents are of analytical grade and purchased from Sigma Aldrich and were consumed without any further purification.

Synthesis of LaBaSrCdO_3

Synthesis of Ba and Sr doped La-based perovskite nanocomposite was done following an already reported sol-gel method (Fig. 1) after some modifications [30].

The beaker filled with 50 mL distilled water and was placed on hot plate having magnetic stirrer in it. Solutions (0.05 M) of lanthanum nitrate ($\text{La}(\text{NO}_3)_3 \cdot 6\text{H}_2\text{O}$), barium chloride ($\text{BaCl}_2 \cdot 2\text{H}_2\text{O}$), strontium chloride ($\text{SrCl}_2 \cdot 6\text{H}_2\text{O}$) and cadmium nitrate ($\text{Cd}(\text{NO}_3)_2$) were added to beaker. Then whole solution was stirred for 8–10 min and then 0.125 M of citric acid and NH_4OH solution (10 % w/w) was poured drop wise to maintain pH 10. Temperature of the resulting mixture was allowed to increase up to 180 °C. Then xerogel was obtained after about 1 h under continuously heating and stirring accompanied by dried in oven at 100 °C for 2 h. The dried, powdered sample was washed with distilled water twice in centrifuge machine and 1 time with ethanol. Then sample was taken in china dish and again dried for 2 h at 100 °C. The synthesized sample was calcined in muffle furnace at 300 °C for 3 h to remove volatile substances and impurities.

Characterization

The functionalities of the prepared materials were monitored using FTIR analysis, which was performed in 4000–400 cm^{-1} range at room temperature and KBr pellets (IR-TRACER-100) [31]. Synthesized nanocomposites were analyzed using XRD (Bruker D8 advance X-ray Diffractometer) with $\text{CuK}\alpha$ (0.154 nm) as a radiation source in 2θ range

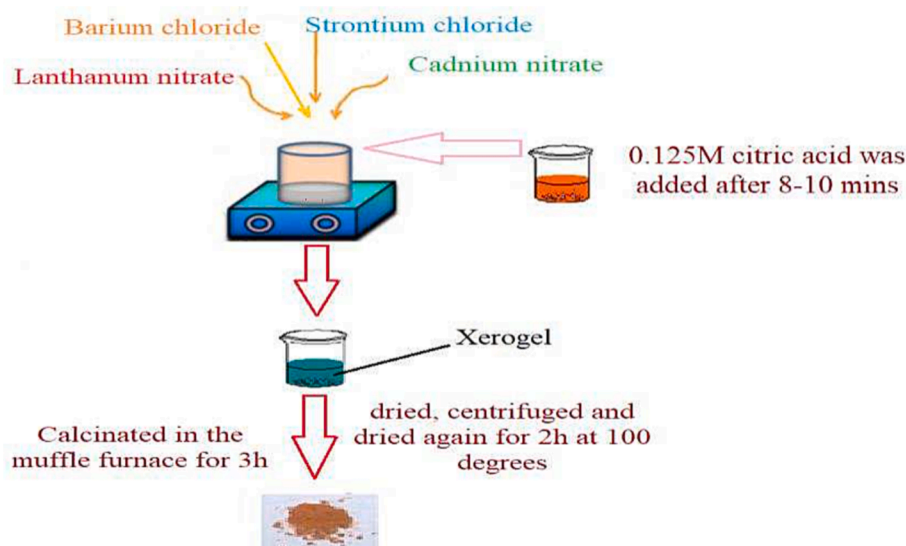


Fig. 1. Synthesis of Ba and Sr doped La-based perovskite nanocomposite.

of 20°–60°. Automatic JCPDS library was used identification purposes [32].

Dielectric studies

The prepared materials dielectric permittivity and electrical resistivity was appraised using Keysight impedance analyzer (E4990A) in 100 Hz–5 MHz and 20–200 °C range. For electrical measurements, the pallets of ~10 mm and ~2 mm by applying 5000 kg/cm² uniaxial pressure by hydraulic press, which were sintered for 6 h at 1300 °C and cooled down 25 °C. The pellets are coated with silver paste and kept at for 30 min at 500 °C and then, subjected to dielectric studies [33,34].

Photocatalytic degradation

Dye degradation studies under UV light were conducted following already reported methods [8,35]. Solutions of Methylene blue (0.05 mM), NaBH₄ (20 mM) and nanocomposite (10, 15, 20 mg/L) were prepared. In a test tube, 3 mL methylene blue (substrate), 0.3 mL NaBH₄ (reducing agent) were mixed. In this resulting solution, 0.5 mL of nanocomposite solution (catalyst) was added. All the observations were recorded at 665 nm (λ^{max} MB). Effect of catalyst dose on dye degradation was determined using different concentration (10 mg, 15 mg and 20 mg) solutions of nanocatalyst. Percentage degradation of MB was calculated and pH optimization was carried out by adjusting the pH of the reaction mixture at 3, 6, and 9.

Results and discussion

FT-IR analysis

Vibrational band analysis of synthesized perovskites sample was done via FT-IR as shown in Fig. 2. The characteristics peaks observe in FT-IR spectrum at 510–850 cm⁻¹, due to stretching vibrations of M–O bond. Therefore, it has been confirmed that prepared sample contain metal oxygen linkages (La–O, Ba–O, Cd–O and Sr–O). Moreover, it is also noted that the bending and stretching mode of the OH bond of water has been showed in the FT-IR spectrum around 1500 and 3485 cm⁻¹, respectively. Thus, FT-IR analysis has confirmed the presence of metal oxygen linkage formed in sample [36].

XRD studies

The XRD spectrum of the synthesized perovskites was recorded using Bruker D8 advanced diffractometer of Cu- K α (0.154 nm) having the range of 2 θ = 20–60° to calculate the average crystallite basal planes

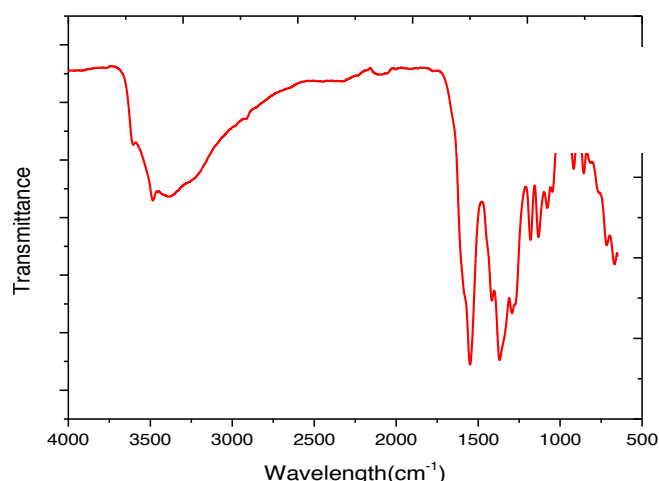


Fig. 2. FTIR Spectrum of Ba and Sr doped La-based perovskite nanocomposite.

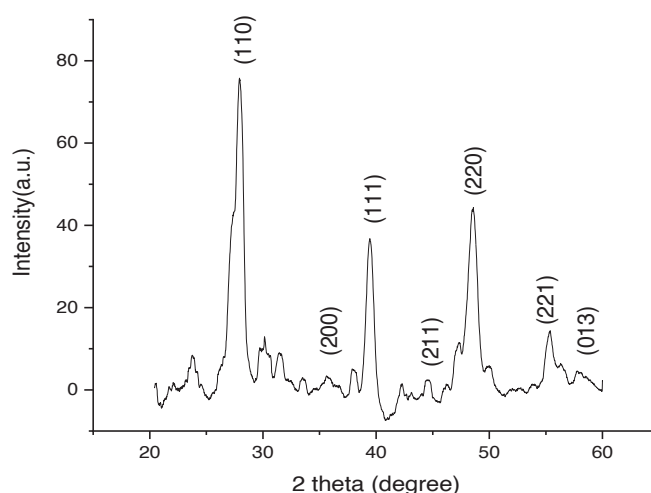


Fig. 3. XRD patron of Ba and Sr doped La-based perovskite nanocomposite.

(Fig. 3) [37]. The spectrum indicates that diffraction peaks at 2 θ = 27.9°, 35.8°, 39.5°, 44.3°, 48.7°, 55.4° and 58.3° correspond to the planes (110), (200), (111), (211), (220), (210), and (013) which confirmed the formation of perovskite and also verify its orthorhombic structure and all the peaks were found perfectly match with JCPDS-00-15-1691. Diffraction peak appeared at 27.9 has confirmed the structure of perovskites. The diffraction peak at 35.8° has confirmed the presence of Sr in sample. The substitution of Ba decreases the crystallinity and the main reflection of the (110) plane would have been moved toward lower angle. This is because when larger Ba²⁺ (radii 0.135 nm) substitute smaller La³⁺ (0.106 nm) in the cubic perovskite structure and thus help in increasing volume of the unit cell [38]. Thus, with the help of XRD analysis, structure of sample and orientation of basal planes has been explained.

The average crystallites size of synthesized perovskites has been measured by Scherrer's formula; $D = K\lambda/\beta\cos\theta$, Where D is particle size in nanometer, K is Scherrer's constant whose value is 0.9, λ is X ray wavelength (1.541), θ = Half of diffraction angle and β is Full width half maxima (FWHM) [39]. Thus, average crystallites size of prepared sample has calculated to be 89.21 nm using Scherrer's formula.

Dielectric studies

The dielectric property of the synthesize perovskite sample was calculated. Alterations in real part of dielectric constant ϵ' with respect to frequency has been studied [40,41]. Dielectric constant was measured using the given formula: $\epsilon' = Cd/A\epsilon_0$, where C donates the capacitance of the material, A shows an area of pallets, width of pallets is represented by d and ϵ_0 is constant which is free space permittivity. The effect of frequency on dielectric constant is shown in Fig. 4a and it reveals that dielectric constant decreases with increasing frequency. The substitution of Ba and Sr introduced inhomogeneity in the structure of perovskite and also reduced the number of moving charges resulting in maximum dielectric constant value at lower frequency. The results of current study were found in agreement with already reported studies [42,43].

The imaginary part of dielectric constant i.e. ϵ'' of synthesized perovskite has been presented in Fig. 4b. The capacitance of the perovskite is elaborated by ϵ' and ϵ'' which gives information regarding dissipation of energy. Imaginary part of dielectric constant i.e. ϵ'' depends on tangent losses and it is calculated using given formula: $\epsilon'' = \epsilon' \times \tan\delta$, where real part of dielectric constant is expressed by the ϵ' . It is explained that dielectric losses are inversely related to frequency and dielectric losses express the amount of dissipated energy. In current study results confirmed that substitution has increased dielectric

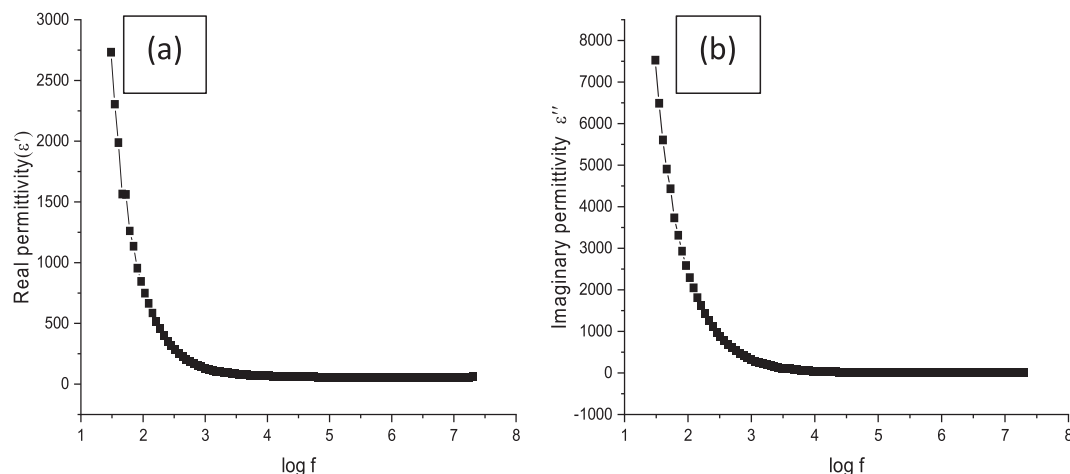


Fig. 4. Effect of frequency on Real dielectric constant (a) and dielectric loss constant (b) of Ba and Sr doped La-based perovskite nanocomposite.

properties that reduced the losses with an increase in frequency. Researchers are designing different material to reduce dielectric losses in terms of dissipated energy. Current study, doping of perovskite favored reduction in losses with respect of increase in frequency and the same already reported in different studies [44,45].

Tangent loss

Tangent loss can be evaluated by using formula $\tan\delta = 1/2\pi fRC$, where f represents applied frequency, resistance of the material is represented by R and C shows the capacitance of the material. The results of tangential loss (Fig. 5) were found inversely related to f and become constant at highest frequency. This process can be elaborated by Koopmans' theory that may help in elucidating the structure of dielectric sample. A net polarization occurred at lower frequency because charges easily align themselves in direction of applied electric field. But at higher frequency tangent loss decrease due to low polarization [46] and it is sign that favors the doping of Ba and Sr in La-based perovskite.

AC conductivity

AC conductivity of the synthesized perovskite sample is calculated by

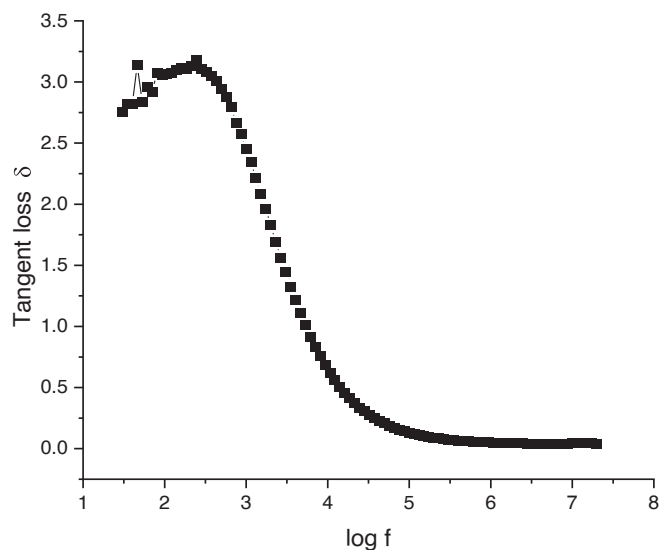


Fig. 5. Effect of frequency on Tangent loss of Ba and Sr doped La-based perovskite nanocomposite.

the given equation. $\rho_{ac} = 1/2\pi f\epsilon''\epsilon_0$ where ' f ' represents frequency, ' ϵ_0 ' shows permittivity of free space and dielectric loss constant is represented by ' ϵ'' '. The results revealed (Fig. 6) that the conductivity of the material is directly related to frequency. This is because substitution of Sr and Ba enhance the charge storage capacity of perovskite due to which its conductivity increased. Results are comparable with the already reported many studies that is confirmed positive impact of doping on perovskite structure and properties [47,48].

Photocatalytic degradation potential

Photocatalytic potential of synthesized nanocomposite was evaluated in terms of dye degradation potential [49,50]. For the purpose, photocatalytic degradation of methylene blue (MB) was achieved. Degradation of dye was carried out using different concentration of perovskite sample (10 mg, 15 mg and 20 mg). Significant effect of catalyst dose was recorded in degradation of dyes as shown in Fig. 7a. It was observed that 20 mg catalyst exhibited maximum 47% degradation of dye (MB) while 10 mg and 15 mg degrade dye by 45.29% and 46.47%. Therefore, it was confirmed that percentage degradation increase with increase in amount of catalyst [51]. In current study La-based perovskite were doped with two different metals i.e. Ba and Sr. Work function values for Ba and Sr are 2.5 eV and 2.1 eV respectively and this

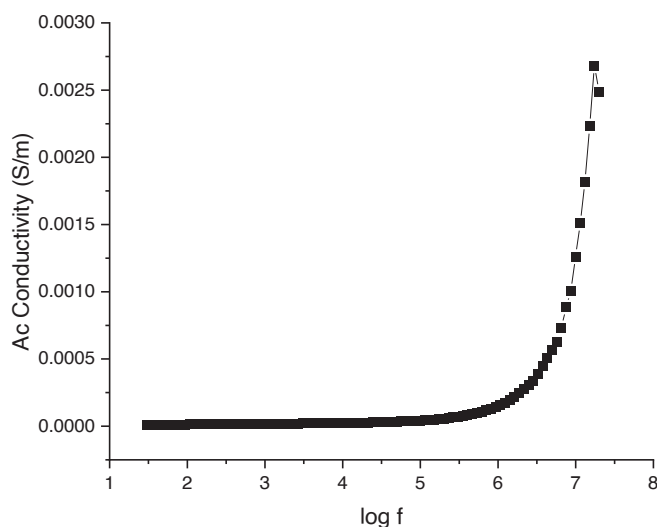


Fig. 6. Effect of frequency on AC conductivity of Ba and Sr doped La-based perovskite nanocomposite.

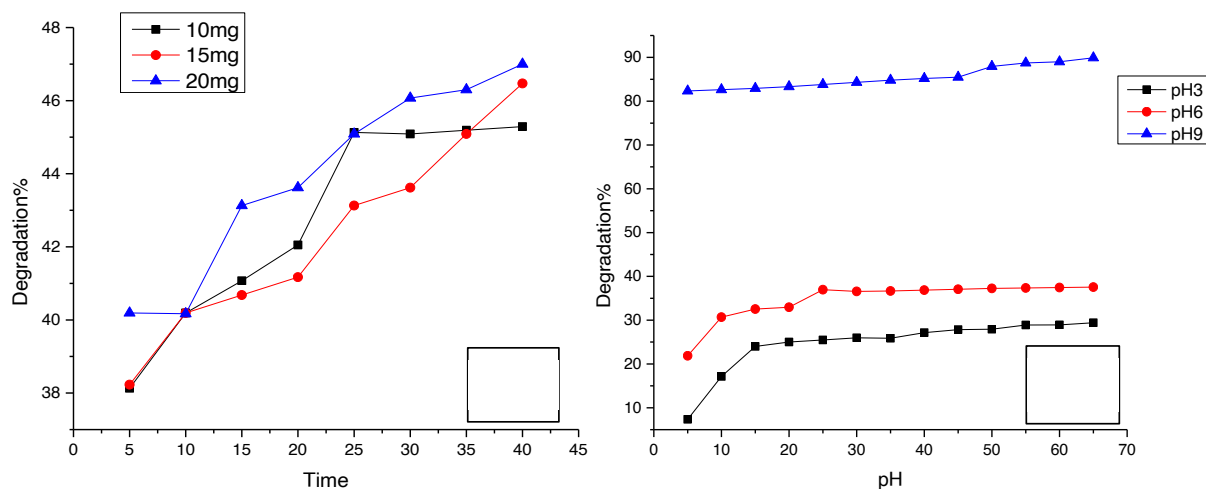


Fig. 7. Effect of catalyst dose (a) and pH (b) on dye degradation potential of Ba and Sr doped La-based perovskite nanocomposite.

difference in work function will allow the movement of electron from lower work function metal to high work function metal. Doping with metals having different work functions will serve as Schottky barrier that will result in movement of electrons necessary for photocatalytic degradation [52]. Carrier diffusion length is another parameter that determine the efficiency of perovskite material. Keeping in view the results of photocatalytic degradation, synthesized perovskite material is expected to have suitable carrier diffusion length suitable and required for catalytic activity [53].

Effect of pH on photocatalytic degradation of MB was studied and change in pH affected the rate of dye degradation. Maximum photocatalytic degradation was observed in basic pH and lesser in acidic medium as shown in Fig. 7b. It is the charge on catalyst that vary due to change in pH and ultimately the degradation of dye [50,54]. The maximum percentage degradation up to 89.92 % was observed at pH 9 and least (29.41%) was observed at pH 3. Maximum degradation has occurred in basic medium because of greater OH radicals' generation that convert methylene blue into less harmful product [55].

Conclusion

Doping is a strategy that is helpful to modify the properties of any material according to need. In current study, Ba and Sr doped La-based perovskites nanocomposite (LaBaSrCdO_3) were fabricated by sol-gel method. Photocatalytic and dielectric properties were demonstrated as a function of doping. Dielectric studies including real/ imaginary dielectric constant, tangent loss and AC conductivity of the synthesis material was determined. Photocatalytic potential of the nanocomposite was tested against MB dye and degradation of the dye was achieved under different conditions of catalyst dose and pH. All the results revealed that doping can enhance the charge storage as well as photocatalytic potential of the nanocomposite. Authors strongly recommend that $\text{La}_x\text{Ba}_{1-x}\text{Sr}_y\text{Cd}_{1-y}\text{O}_{3\pm\delta}$ like nanocomposites should be designed and doping strategy should be adopted to modify the properties of the materials according to the requirement of specific application. In future, different metals, instead of Ba and Sr, can be used for doping to achieve desired characteristics.

CRediT authorship contribution statement

Sadia Ata: Conceptualization, Supervision. **Ifra Shaheen:** Formal analysis, Investigation. **Hira Aslam:** Writing – original draft. **Ijaz Ul Mohsin:** Methodology. **Norah Alwadai:** Formal analysis, Software, Funding acquisition. **Maryam Al Huwayz:** Formal analysis, Validation. **Munawar Iqbal:** Project administration, Resources, Visualization,

Writing - review & editing. **Umer Younas:** Data curation, Writing - original draft, Writing - review & editing.

Research Funding

This research was funded by Princess Nourah bint Abdulrahman University Researchers Supporting Project number (PNURSP2023R11), Princess Nourah bint Abdulrahman University, Riyadh, Saudi Arabia.

Declaration of Competing Interest

The authors declare that they have no known competing financial interests or personal relationships that could have appeared to influence the work reported in this paper.

Data availability

No data was used for the research described in the article.

Acknowledgments

The authors express their gratitude to Princess Nourah bint Abdulrahman University Researchers Supporting Project number (PNURSP2023R11), Princess Nourah bint Abdulrahman University, Riyadh, Saudi Arabia.

References

- [1] Okereke J, Ogidi O, Obasi K. Environmental and health impact of industrial wastewater effluents in Nigeria-A Review. *Int J Adv Res Biol Sci* 2016;3(6):55–67.
- [2] Khan S, Malik A. Environmental and health effects of textile industry wastewater. In *Environmental deterioration and human health*. Springer; 2014. pp. 55–71.
- [3] Jadhav SA, Somvanshi SB, Khedkar MV, Patade SR, Jadhav K. Magneto-structural and photocatalytic behavior of mixed Ni–Zn nano-spinel ferrites: visible light-enabled active photodegradation of rhodamine B. *J Mater Sci Mater Electron* 2020; 31(14):11352–65.
- [4] Shih Y-H, Tso C-P, Tung L-Y. Rapid degradation of methyl orange with nanoscale zerovalent iron particles. *Nanotechnology* 2010;7(16):7.
- [5] Kusic H, Koprivanac N, Srsan L. Azo dye degradation using Fenton type processes assisted by UV irradiation: a kinetic study. *J Photochem Photobiol A Chem* 2006; 181(2–3):195–202.
- [6] Chung K-T. Azo dyes and human health: A review. *J Environ Sci Health C* 2016;34(4):233–61.
- [7] Katheresan V, Kansedo J, Lau SY. Efficiency of various recent wastewater dye removal methods: A review. *J Environ Chem Eng* 2018;6(4):4676–97.
- [8] Younas U, Hassan ST, Ali F, Hassan F, Saeed Z, Pervaiz M, et al. Radical scavenging and catalytic activity of Fe-Cu bimetallic nanoparticles synthesized from *Ixora finlaysoniana* extract. *Coatings* 2021;11(7):813.
- [9] Somvanshi SB, Somvanshi SB, Kharat PB, Thorat ND. Magnetically Retrievable Fe-Doped TiO₂ Nanoparticles for Photo-induced Toxic Dye Removal Applications. In *Macromolecular Symposia*. Wiley Online Library; 2021. p. 2100112.

- [10] Tavakkoli H, Beiknejad D, Tabari T. Fabrication of perovskite-type oxide La_{0.5}Ca_{0.5}CoO_{3-δ} nanoparticles and its dye removal performance. *Desalin Water Treat* 2014;52(37–39):7377–88.
- [11] Shahzad U. The need for renewable energy sources. *Energy* 2012;2:16–8.
- [12] Zhang J, Zhang G, Zhou T, Sun S. Recent developments of planar micro-supercapacitors: fabrication, properties, and applications. *Adv Funct Mater* 2020;30(19):1910000.
- [13] Zhang B, Wan Y, Hua Z, Tang K, Xia C. Tungsten-doped PrBaFe₂O_{5+δ} double perovskite as a high-performance electrode material for symmetrical solid oxide fuel cells. *ACS Appl Energy Mater* 2021;4(8):8401–9.
- [14] Devmunde B, Somvanshi SB, Kharat PB, Solunke MB. Rare Earth Ion (La³⁺) Doped BaTiO₃ Perovskite Nanoceramics for Spintronic Applications. In *Journal of Physics: Conference Series*. IOP Publishing; 2020. p. 012055.
- [15] Fan H, Zhang X, Wang Y, Gao R, Lang J. Mn and Co co-doped perovskite fluorides KNiF₃ with enhanced capacitive performance. *J Colloid Interface Sci* 2019;557:546–55.
- [16] Lu C-H, Biesold-McGee GV, Liu Y, Kang Z, Lin Z. Doping and ion substitution in colloidal metal halide perovskite nanocrystals. *Chem Soc Rev* 2020;49(14):4953–5007.
- [17] Bhojar DN, Somvanshi SB, Kharat PB, Pandit A, Jadhav K. Structural, infrared, magnetic and ferroelectric properties of Sr_{0.5}Ba_{0.5}Ti_{1-x}Fe_xO₃ nanoceramics: Modifications via trivalent Fe ion doping. *Phys B Condens Matter* 2020;581:411944.
- [18] Musialik-Piotrowska A, Landmesser H. Noble metal-doped perovskites for the oxidation of organic air pollutants. *Catal Today* 2008;137(2–4):357–61.
- [19] Yang J, Guo Y. Nanostructured perovskite oxides as promising substitutes of noble metals catalysts for catalytic combustion of methane. *Chin Chem Lett* 2018;29(2):252–60.
- [20] Singh UG, Li J, Bennett JW, Rappe AM, Seshadri R, Scott SL. A Pd-doped perovskite catalyst, BaCe_{1-x}Pd_xO_{3-δ}, for CO oxidation. *J Catal* 2007;249(2):349–58.
- [21] Ghiasi M, Malekzadeh A. Solar photocatalytic degradation of methyl orange over La_{0.7}Sr_{0.3}MnO₃ nano-perovskite. *Sep Purif Technol* 2014;134:12–9.
- [22] Esmaili S, Ehsani M, Fazli M. Structural, optical and photocatalytic properties of La_{0.7}Ba_{0.3}MnO₃ nanoparticles prepared by microwave method. *Chem Phys* 2020;529:110576.
- [23] Kumar SR, Abinaya C, Amirthapandian S, Ponpandian N. Enhanced visible light photocatalytic activity of porous LaMnO₃ sub-micron particles in the degradation of rose bengal. *Mater Res Bull* 2017;93:270–81.
- [24] Mefford JT, Hardin WG, Dai S, Johnston KP, Stevenson KJ. Anion charge storage through oxygen intercalation in LaMnO₃ perovskite pseudocapacitor electrodes. *Nat Mater* 2014;13(7):726–32.
- [25] Mahmood A, Warsi MF, Ashiq MN, Sher M. Improvements in electrical and dielectric properties of substituted multiferroic LaMnO₃ based nanostructures synthesized by co-precipitation method. *Mater Res Bull* 2012;47(12):4197–202.
- [26] Borade RM, Somvanshi SB, Kale SB, Pawar RP, Jadhav K. Spinel zinc ferrite nanoparticles: an active nanocatalyst for microwave irradiated solvent free synthesis of chalcones. *Mater Res Express* 2020;7(1):016116.
- [27] Wenwei W, Jinchao C, Xuehang W, Sen L, Kaituo W, Lin T. Nanocrystalline LaMnO₃ preparation and kinetics of crystallization process. *Adv Powder Technol* 2013;24(1):154–9.
- [28] Khirade PP, Chavan AR, Somvanshi SB, Kounsalye JS, Jadhav K. Tuning of physical properties of multifunctional Mg-Zn spinel ferrite nanocrystals: a comparative investigations manufactured via conventional ceramic versus green approach sol-gel combustion route. *Mater Res Express* 2020;7(11):116102.
- [29] Danks AE, Hall SR, Schnepf Z. The evolution of 'sol-gel' chemistry as a technique for materials synthesis. *Mater Horiz* 2016;3(2):91–112.
- [30] Azouzi W, Sigle W, Labrim H, Benaissa M. Sol-gel synthesis of nanoporous LaFeO₃ powders for solar applications. *Mater Sci Semicond Process* 2019;104:104682.
- [31] Somvanshi SB, Patade SR, Andhare DD, Jadhav SA, Khedkar MV, Kharat PB, et al. Hyperthermic evaluation of oleic acid coated nano-spinel magnesium ferrite: enhancement via hydrophobic-to-hydrophilic surface transformation. *J Alloy Compd* 2020;835:155422.
- [32] Aman D, Zaki T, Mikhail S, Selim S. Synthesis of a perovskite LaNiO₃ nanocatalyst at a low temperature using single reverse microemulsion. *Catal Today* 2011;164(1):209–13.
- [33] Kumar D, Jena P, Singh AK. Structural, magnetic and dielectric studies on half-doped Nd_{0.5}Ba_{0.5}CoO₃ perovskite. *J Magn Magn Mater* 2020;516:167330.
- [34] Coskun M, Polat O, Coskun F, Kurt BZ, Durmus Z, Caglar M, et al. The impact of Ir doping on the electrical properties of YbFe_{1-x}Ir_xO₃ perovskite-oxide compounds. *J Mater Sci Mater Electron* 2020;31(2):1731–44.
- [35] Younas U, Gulzar A, Ali F, Pervaiz M, Ali Z, Khan S, et al. Antioxidant and Organic Dye Removal Potential of Cu-Ni Bimetallic Nanoparticles Synthesized Using *Gazania rigens* Extract. *Water* 2021;13(19):2653.
- [36] Kolat V, Gencer H, Gunes M, Atalay S. Effect of B-doping on the structural, magnetotransport and magnetocaloric properties of La_{0.67}Ca_{0.33}MnO₃ compounds. *Mater Sci Eng B* 2007;140(3):212–7.
- [37] Humbe AV, Kounsalye JS, Somvanshi SB, Kumar A, Jadhav K. Cation distribution, magnetic and hyperfine interaction studies of Ni-Zn spinel ferrites: role of Jahn Teller ion (Cu²⁺) substitution. *Mater Adv* 2020;1(4):880–90.
- [38] Wang J, Su Y, Wang X, Chen J, Zhao Z, Shen M. The effect of partial substitution of Co in LaMnO₃ synthesized by sol-gel methods for NO oxidation. *Catal Commun* 2012;25:106–9.
- [39] Somvanshi SB, Jadhav SA, Khedkar MV, Kharat PB, More S, Jadhav K. Structural, thermal, spectral, optical and surface analysis of rare earth metal ion (Gd³⁺) doped mixed Zn-Mg nano-spinel ferrites. *Ceram Int* 2020;46(9):13170–9.
- [40] More S, Khedkar M, Jadhav S, Somvanshi SB, Humbe A, Jadhav K. Wet chemical synthesis and investigations of structural and dielectric properties of BaTiO₃ nanoparticles. In *Journal of Physics: Conference Series*. IOP Publishing; 2020. p. 012007.
- [41] Bhosale AB, Somvanshi SB, Murumkar V, Jadhav K. Influential incorporation of RE metal ion (Dy³⁺) in yttrium iron garnet (YIG) nanoparticles: Magnetic, electrical and dielectric behaviour. *Ceram Int* 2020;46(10):15372–8.
- [42] Yao Z, Song Z, Hao H, Yu Z, Cao M, Zhang S, et al. Homogeneous/inhomogeneous-structured dielectrics and their energy-storage performances. *Adv Mater* 2017;29(20):1601727.
- [43] Ishaque M, Islam M, Khan MA, Rahman I, Genson A, Hampshire S. Structural, electrical and dielectric properties of yttrium substituted nickel ferrites. *Phys B Condens Matter* 2010;405(6):1532–40.
- [44] El-Mallah H. AC electrical conductivity and dielectric properties of perovskite (Pb, Ca) TiO₃ ceramic. *Acta Phys Pol-Ser A General Phys* 2012;122(1):174.
- [45] Nazir N, Ikram M. Structural, dielectric, and conductivity studies of strontium-doped Gd₂NiMnO₆ perovskite. *J Mater Sci Mater Electron* 2020;31(24):23002–11.
- [46] Padhy M, Dehury SK, Choudhary R, Achary P. Structural, dielectric, thermal and electrical characteristics of lead-free double perovskite: BiHoZnCeO₆. *Appl Phys A* 2020;126(8):1–13.
- [47] Arshad M, Du H, Javed MS, Maqsood A, Ashraf I, Hussain S, et al. Fabrication, structure, and frequency-dependent electrical and dielectric properties of Sr-doped BaTiO₃ ceramics. *Ceram Int* 2020;46(2):2238–46.
- [48] Slimani Y, Unal B, Hannachi E, Selmi A, Almessiere M, Nawaz M, et al. Frequency and dc bias voltage dependent dielectric properties and electrical conductivity of BaTiO₃SrTiO₃/(SiO₂)_x nanocomposites. *Ceram Int* 2019;45(9):11989–2000.
- [49] Akbari A, Sabouri Z, Hosseini HA, Hashemzadeh A, Khatami M, Darroudi M. Effect of nickel oxide nanoparticles as a photocatalyst in dyes degradation and evaluation of effective parameters in their removal from aqueous environments. *Inorg Chem Commun* 2020;115:107867.
- [50] Karami M, Ghanbari M, Amiri O, Salavati-Niasari M. Enhanced antibacterial activity and photocatalytic degradation of organic dyes under visible light using cesium lead iodide perovskite nanostructures prepared by hydrothermal method. *Sep Purif Technol* 2020;253:117526.
- [51] Somvanshi SB, Kharat PB, Khedkar MV, Jadhav K. Hydrophobic to hydrophilic surface transformation of nano-scale zinc ferrite via oleic acid coating: magnetic hyperthermia study towards biomedical applications. *Ceram Int* 2020;46(6):7642–53.
- [52] Fageria P, Gangopadhyay S, Pande S. Synthesis of ZnO/Au and ZnO/Ag nanoparticles and their photocatalytic application using UV and visible light. *RSC Adv* 2014;4(48):24962–72.
- [53] Chen B, Baek S-W, Hou Y, Aydin E, De Bastiani M, Scheffel B, et al. Enhanced optical path and electron diffusion length enable high-efficiency perovskite tandems. *Nat Commun* 2020;11(1):1–9.
- [54] Jadhav SA, Khedkar MV, Somvanshi SB, Jadhav K. Magnetically retrievable nanoscale nickel ferrites: an active photocatalyst for toxic dye removal applications. *Ceram Int* 2021;47(20):28623–33.
- [55] Rani M, Shanker U. Sun-light driven rapid photocatalytic degradation of methylene blue by poly (methyl methacrylate)/metal oxide nanocomposites. *Colloids Surf A* 2018;559:136–47.